The Plant Cell, Vol. 18, 1383–1395, June 2006, www.plantcell.org

GLABROUS INFLORESCENCE STEMS Modulates the Regulation by Gibberellins of Epidermal Differentiation and Shoot Maturation in *Arabidopsis* [W]

Yinbo Gan,[a] Rod Kumimoto,[b] Chang Liu,[c] Oliver Ratcliffe,[b] Hao Yu,[c] and Pierre Broun[a,1]

[a] Centre for Novel Agricultural Projects, Department of Biology, University of York, York YO10 5YW, United Kingdom
[b] Mendel Biotechnology, Hayward, California 94545
[c] Department of Biological Sciences and Temasek Life Sciences Laboratory, National University of Singapore, Singapore 117543

As a plant shoot matures, it transitions through a series of growth phases in which successive aerial organs undergo distinct developmental changes. This process of phase change is known to be influenced by gibberellins (GAs). We report the identification of a putative transcription factor, GLABROUS INFLORESCENCE STEMS (GIS), which regulates aspects of shoot maturation in *Arabidopsis thaliana*. GIS loss-of-function mutations affect the epidermal differentiation of inflorescence organs, causing a premature decrease in trichome production on successive leaves, stem internodes, and branches. Overexpression has the opposite effect on trichome initiation and causes other heterochronic phenotypes, affecting flowering and juvenile–adult leaf transition and inducing the formation of rosette leaves on inflorescence stems. Genetic and gene expression analyses suggest that GIS acts in a GA-responsive pathway upstream of the trichome initiation regulator GLABROUS1 (GL1) and downstream of the GA signaling repressor SPINDLY (SPY). GIS mediates the induction of GL1 expression by GA in inflorescence organs and is antagonized in its action by the DELLA repressor GAI. The implication of GIS in the broader regulation of phase change is further suggested by the delay in flowering caused by GIS loss of function in the *spy* background. The discovery of GIS reveals a novel mechanism in the control of shoot maturation, through which GAs regulate cellular differentiation in plants.

INTRODUCTION

Organ initiation in plants, in contrast with animals, takes place through much of the life cycle. Successive organs may, however, develop distinctive morphological and physiological characteristics that are dependent on the developmental stage of the plant at the time the organ primordia are fated. This maturation process occurs both before and after the plant develops reproductive competence. During embryogenesis, the shoot apex produces embryonic leaves or cotyledons, which contrast with postembryonic leaves in their morphology and role in storage reserve accumulation. After germination, successive leaves go through a juvenile phase before adopting an adult form, a process termed vegetative phase change, which is largely age dependent but independent of growth rate (Telfer et al., 1997). Shoot maturation also affects leaves that are generated as the plant is committed to flowering, and their pattern of differentiation is thought to depend on the developmental state of corresponding primordia in the shoot apex at the time of floral induction (Hempel and Feldman, 1994; Telfer et al., 1997). In *Arabidopsis thaliana*, the changing distribution of trichomes, which are spiky epidermis-derived structures at the surface of aerial organs, is a robust morphological marker of phase change. During vegetative development, juvenile leaves only develop trichomes on their upper (adaxial) side, whereas adult leaves produce trichomes on their adaxial and lower (abaxial) sides. After flowering, trichomes forming on the adaxial side of inflorescence leaves (cauline leaves) follow a contrasting pattern of initiation and are gradually less abundant on successive leaves (Telfer et al., 1997).

Phase change and trichome distribution are known to be influenced by gibberellins (GAs). In maize (*Zea mays*), GAs promote the expression of adult traits, in particular trichome production, during the vegetative phase (Evans and Poethig, 1995). In *Arabidopsis*, loss-of-function mutations impairing GA biosynthesis or sensitivity delay the appearance of adult leaves. By contrast, exogenous GA applications accelerate the transition from juvenile to adult phase (Chien and Sussex, 1996; Telfer et al., 1997). In the embryo, the retention of embryonic characteristics by cotyledons is also thought to implicate GAs (Gazzarrini et al., 2004). In relation to their role in phase change, GAs are known to affect the expression of *GLABROUS1* (*GL1*), which encodes a MYB transcription factor that is a core component of a complex necessary for *Arabidopsis* trichome initiation (Perazza et al., 1998). The trichome initiation complex also comprises the basic helix-loop-helix transcription factors GL3 and ENHANCER of GL3 (EGL3) and the WD40 protein TRANSPARENT TESTA

[1] To whom correspondence should be addressed. E-mail pb22@york.ac.uk; fax 44-1904-328762.
The author responsible for distribution of materials integral to the findings presented in this article in accordance with the policy described in the Instructions for Authors (www.plantcell.org) is: Pierre Broun (pbroun@york.ac.uk).
[W] Online version contains Web-only data.
Article, publication date, and citation information can be found at www.plantcell.org/cgi/doi/10.1105/tpc.106.041533.

GLABRA1 (TTG1); the transcriptional effects of GAs on GL1 may be important for modulating the activity of the initiation complex as a whole (Larkin et al., 1994; Walker et al., 1999; Payne et al., 2000; Zhang et al., 2003). Despite the growing body of information relating to the regulation of vegetative phase change (Telfer and Poethig, 1998; Clarke et al., 1999; Groot and Meicenheimer, 2000; Berardini et al., 2001; Prigge and Wagner, 2001; Hunter et al., 2003), the molecular mechanisms through which GAs regulate different aspects of shoot maturation in adult plants, in particular trichome initiation, are unknown.

We report here the identification of a putative C2H2 transcription factor, which modulates the regulation of shoot maturation by GAs, and show that it plays a central role in epidermal differentiation through its influence on GL1 activity.

RESULTS

Overexpression of *GLABROUS INFLORESCENCE STEMS* in *Arabidopsis* Stimulates Trichome Initiation and Causes the Heterochronic Expression of Juvenile Traits

In an effort to uncover novel functions of transcription factors in plants, a genome-wide reverse genetics analysis of gain-of-function phenotypes was conducted at Mendel Biotechnology across different *Arabidopsis* transcription factor families (Riechmann et al., 2000). This experiment identified novel genes that play a role in the control of developmental phase change and trichome production. Among them, *GLABROUS INFLORESCENCE STEMS* (*GIS*; corresponding to At3g58070) was first uncovered by screening transgenic *Arabidopsis* plants overexpressing transcription factor genes. Multiple independent *35S*:*GIS* overexpression lines displayed an abnormally high density of trichomes on inflorescence organs (Figures 1A and 1B). Two representative lines were selected for detailed studies: line 6 and line 8, which exhibited high and moderate levels, respectively, of *GIS* overexpression (81- and 18-fold wild-type levels). In both of these lines, the distribution of trichomes on cauline leaves was significantly altered: instead of decreasing in numbers on the adaxial side of successive leaves, trichomes remained unusually abundant, which suggested that progression of the epidermal differentiation program was delayed. In lines 6 and 8, the average adaxial trichome density on the second cauline leaf was 68 and 45% higher, respectively, than in control plants (Figure 2F). Significantly more trichomes were also noticeable on stems and sepals in the overexpressors. In addition to suppressing the progressive decline in trichome production, *GIS* overexpression caused the formation of ectopic trichomes on carpels, petals, and even stamens (Figure 1B). By contrast, trichome density was normal on rosette leaves of *35S*:*GIS* lines (Figure 2F).

35S:*GIS* plants also displayed a number of phenotypic changes that we interpreted as heterochronic shifts in development. For example, *35S*:*GIS* plants flowered significantly later than wild-type plants, after producing more leaves (Table 1). *GIS* overexpression also caused the occasional appearance of aerial rosettes on the inflorescence stems of transgenic plants, in place of cauline leaves (Figure 1C).

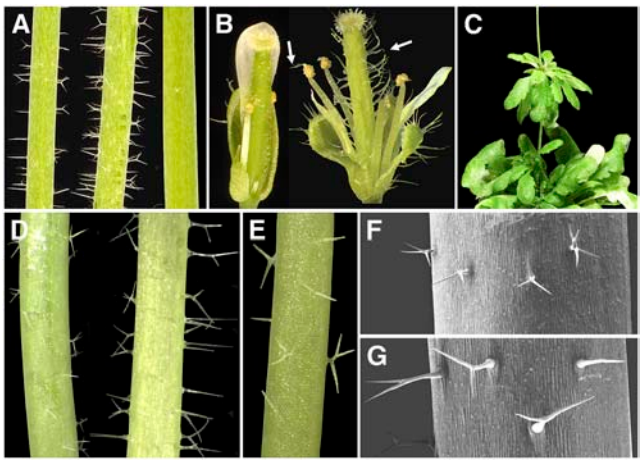

Figure 1. Phenotype of Loss-of-Function *gis* Mutants and 35S:*GIS* Overexpressors.

(A) Main inflorescence stems (2nd internode) of the wild type (left), 35S:*GIS* transgenic line 8 (center), and *gis* (right).
(B) Exposed floral organs from a wild-type (left) and 35S:*GIS* (right) dissected flower. Arrows point to ectopic trichomes.
(C) Rosette formation on the primary inflorescence stem of a strong *GIS* overexpressor.
(D) Comparison inflorescence stems of a complemented *35S*:*GIS gis* line (right) and *gis* (left).
(E) Trichomes on an inflorescence stem (2nd internode) of a transgenic plant in which *GIS* has been silenced by RNAi (line *GIS-Ri-1*).
(F) and **(G)** Trichome branching pattern on *gis* **(F)** and control stems **(G)**. Note that *gis* trichomes are smaller and more branched than their wild-type counterparts.

In summary, *GIS* overexpressors displayed a phenotype consistent with a delay in shoot maturation, associated with a strong induction of trichome production on the inflorescence.

GIS Loss-of-Function Affects the Timing of Trichome Initiation on Inflorescence Organs

To test whether the true biological function of *GIS* is to mediate morphological changes associated with phase change, we obtained, from the GABI-Kat library of insertional mutants (Rosso et al., 2003), a line in which *GIS* is interrupted by a T-DNA insertion. Presence of the T-DNA at the expected location was verified by genomic PCR, and *GIS* expression was undetectable based on quantitative PCR analysis (see Supplemental Figure 1A online).

We focused our initial analysis on trichome production in the mutant. The pattern of trichome initiation is well documented for leaves but not for other aerial organs. To better assess the possible role played by GIS in epidermal differentiation, we first characterized in detail trichome distribution on stems, paraclades (secondary inflorescence shoots or branches), and flowers in wild-type plants. In addition to the known decline in adaxial trichome production on successive inflorescence leaves (Telfer et al., 1997), we observed that trichome initiation decreases on successive stem internodes, branches, and flowers (Figures 2A to 2D). Overall, we found a striking correlation between trichome

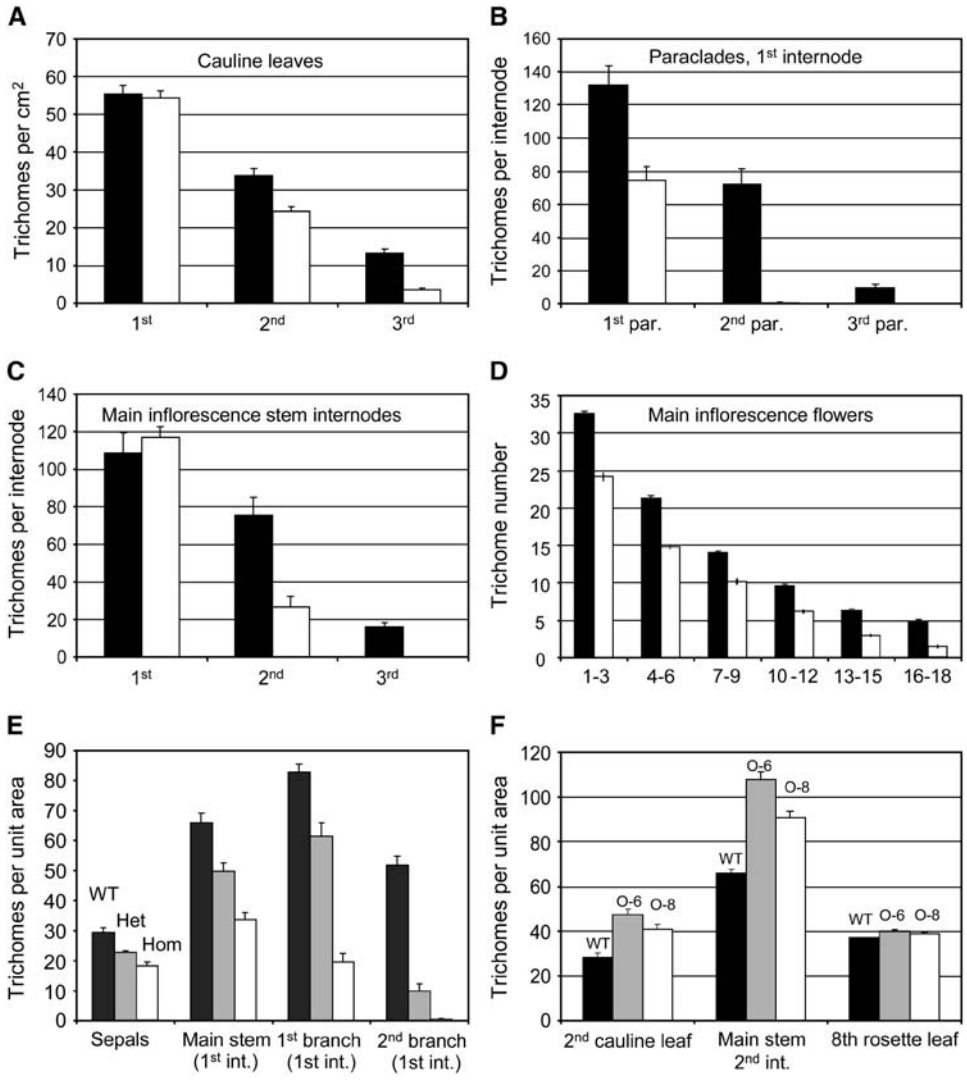

Figure 2. Trichome Initiation on Inflorescence Organs of *gis* Mutants and *35S:GIS* Overexpressing Lines.

(A) to **(D)** Trichome density in *gis* and wild-type plants **(A)**, first internodes of successive paraclades **(B)**, main stem internodes **(C)**, and sepals **(D)**. Flower trichome counts represent the total for 20 flowers. Values are averages, and error bars correspond to standard error. Black bars, wild type; white bars, *gis* mutant; par., paraclade.

(E) Trichome density on inflorescence organs in *gis* homozygotes and *gis*/+ heterozygotes. Dark gray bars, wild-type controls; gray bars, heterozygotes (Het.); white bars, homozygotes (Hom.).

(F) Trichome density on inflorescence organs and on rosette leaves in *35S*:*GIS*-overexpressing lines. O-6, *35S*:*GIS*-overexpressing line 6; O-8, *35S*:*GIS*-overexpressing line 8; int., internode.

density and distance from the base of the inflorescence (see Supplemental Figure 2 online).

In contrast with the overexpression phenotype, trichome initiation was negatively affected on all inflorescence organs in *gis* mutants, and the effect was stronger in later than in earlier organs (Figures 2A to 2D). The reduction in trichome density was most noticeable on paraclade stems (branches), which were near-glabrous or glabrous (hence the gene name), and was also detectable on main stem internodes and cauline leaves, mostly above the first branch. The flowers of *gis* followed a similar trend, with a more steady decrease in trichome density. The number of branches or spikes on trichomes was also affected in the mutant. In contrast with wild-type stems, where most trichomes possessed one or two branches, an average 85% of the trichomes on *gis* stems had three branches and were more similar in this respect to leaf trichomes (Figure 1F). Such an increase in trichome branching was also observed on rosette leaves, most noticeably on their abaxial side (data not shown). However, in contrast with inflorescence organs, rosette leaves produced a normal number of trichomes in the mutant (see below). In

Table 1. Effect of *GIS* Loss of Function and Overexpression on Plant Growth and Development

	Height at Maturity (cm)	Rosette Leaf Size (mm^2; 8th leaf)	First Leaf with Abaxial Trichomes	Rosette Leaf Number at Flowering		Flowering Time (d)	
				LD	SD	LD	SD
Wild type	41.0 (0.6)	540.4 (7.2)	6.4 (0.1)	12.3 (0.1)	30.5 (0.6)	27.2 (0.2)	53.4 (0.3)
gis	40.9 (0.6)	549.2 (11.1)	6.5 (0.1)	12.4 (0.1)	30.8 (0.3)	27.0 (0.2)	52.8 (0.4)
Wild type	–	–	6.4 (0.1)	11.6 (0.4)	–	26.6 (0.3)	–
O-6	–	–	7.8 (0.1)	18.8 (0.3)	–	38.2 (0.7)	–
O-8	–	–	7.4 (0.1)	16.1 (0.6)	–	30.1 (0.6)	–
Wild type	–	–	6.3 (0.1)	11.9 (0.1)	–	27.5 (0.2)	–
gis	–	–	6.3 (0.2)	11.8 (0.2)	–	27.7 (0.1)	–
spy-3	–	–	3.8 (0.1)	8.3 (0.1)	–	25.2 (0.2)	–
gis spy	–	–	4.6 (0.1)	9.8 (0.2)	–	27.0 (0.2)	–
gis/+ *spy*	–	–	4.4 (0.2)	9.1 (0.2)	–	26.1 (0.3)	–

Values are averages and standard errors. LD, long days; SD, short days; O-6, *35S*:*GIS*-overexpressing line 6; O-8, *35S*:*GIS*-overexpressing line 8.

addition, unlike some of the trichome initiation mutants, *gis* did not exhibit any obvious defect in anthocyanin, root hair, or mucilage production (data not shown).

As *GIS* overexpression not only affected trichome production, but also induced other heterochronic phenotypes, we examined the process of shoot maturation in the mutant. We found that the mutation did not affect flowering time in long or short days, the rate of leaf initiation, or plant size (Table 1). We also examined leaf shape and venation patterns during vegetative and inflorescence development but did not find any significant difference between *gis* and wild-type plants. Therefore, in contrast with overexpression, *GIS* loss of function mainly affected epidermal differentiation after floral induction under normal conditions.

To verify the *GIS* loss-of-function phenotype, we generated multiple transgenic lines in which the *GIS* gene was silenced by an RNA interference (RNAi)–based approach (see Supplemental Figure 1B online); most of these lines showed a phenotype comparable to that of the T-DNA mutant (Figure 1E). As a further verification that the phenotype was caused by the *GIS* loss-of-function mutation and not by another linked mutation, we overexpressed *GIS* under the control of the 35S promoter in the *gis* T-DNA line background. Constitutive overexpression rescued the mutant phenotype in most lines, also causing an increasing in trichome density on flowers and on stems (Figure 1D).

The *gis* Mutation Is Semidominant

To determine the influence of gene dosage on the trichome phenotype, we analyzed an F2 population derived from a *gis*/+ plant. The genotype of segregating progenies was determined using genomic PCR (data not shown), and their phenotype was analyzed. In line with our expectations, we found that all lines homozygous for the T-DNA insertion were defective in trichome initiation. By contrast, all of the plants homozygous for the wild-type allele were found to have a normal trichome phenotype. Heterozygous plants also showed a marked decrease in trichome density and displayed a phenotype that was intermediate between wild-type and homozygous plants (Figure 2E). This observation indicated that the *gis* mutation is semidominant and that relatively small variations in *GIS* expression can have a dramatic effect on the processes that the gene controls.

GIS Acts Upstream of the Trichome Initiation Complex

Since trichome initiation is affected in *gis* and the overexpressor, we investigated the position of GIS in the trichome initiation pathway and overexpressed the *GIS* gene in the *gl1*, *gl3*, and *ttg-1* mutant backgrounds. Trichome initiation was not rescued by *GIS* overexpression in *gl1*, *gl3* (Figures 3A and 3B), or *ttg-1* (data not shown). In a complementary experiment, we asked whether the trichome defect of *gis* mutants could be overcome by increased activity of the trichome initiation complex. To test this possibility, we overexpressed, in the *gis* mutant background, the maize basic helix-loop-helix regulator R, which is known to be functionally equivalent to trichome initiation regulators GL3 and EGL3 in *Arabidopsis* (Lloyd et al., 1992). Expression of *R* under the control of the 35S promoter led to a strong increase in leaf and stem trichome initiation in transgenic plants (Figure 3C). Taken together, these results suggested that GIS acts either upstream or at the same step as GL1, TTG1, and GL3.

To further assess the functional relationship between GIS and trichome initiation regulators, we measured the expression level of *GL1*, *GL3*, and *EGL3* in developing stems and flowers of the *gis* mutant. As shown in Figure 4, the expression of *GL1*, *GL3*, and *EGL3* was significantly lower in the mutant than in wild-type controls. The difference was not simply the result of a decrease in the production of trichomes, where these genes are also expressed, since no significant difference in *GL1* expression could be detected in *ttg-1* (which is completely glabrous) and since *GL3* is upregulated in this mutant (Zhang et al., 2003) (Figure 4). By contrast, we found that the expression of *GL1* and *GL3* was significantly increased in 35S:*GIS* plants and that their induction level correlated with the level of expression of *GIS* overexpression. It was not the case for *TTG1* expression, which was neither affected in the overexpressing lines nor in the mutant (Figure 4). Taken together, these genetic experiments and expression studies argued that GIS acts upstream of the trichome initiation complex.

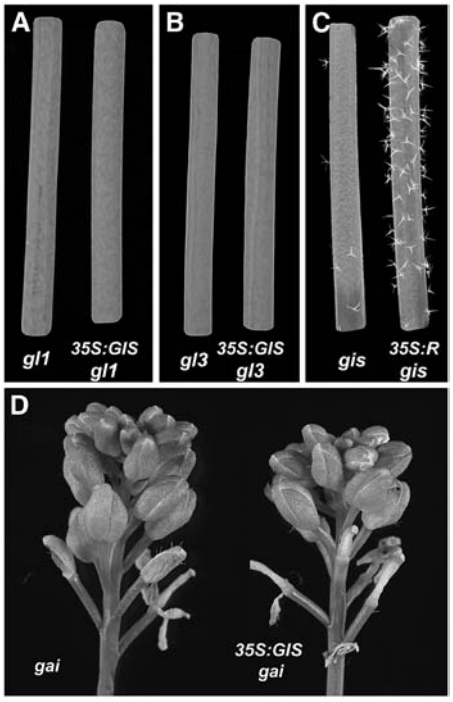

Figure 3. Genetic Interactions between *GIS* and Trichome Initiation Regulatory Genes.

(A) and **(B)** Trichome initiation on main stems (first internode) of *35S*:*GIS* overexpressors in two different mutant backgrounds: *gl1* (left) and *35S*:*GIS gl1* (right) **(A)**; *gl3* (left) and *35S*:*GIS gl3* (right) **(B)**.

(C) Trichome initiation on stems (2nd internode) of *gis* mutants overexpressing the maize *R* gene. *R* overexpression rescues the trichome initiation phenotype of the *gis* mutant.

(D) Effect of the *gai* mutation on the *GIS* overexpression phenotype. Trichome initiation is inhibited in the absence of GA signaling. Left, *gai* flowers; right, *35S*:*GIS gai* flowers.

GIS Encodes a Transcription Factor of the C2H2 Family That Is Highly Expressed in Stem Epidermis and at Early Stages of Inflorescence and Flower Development

Analysis of the predicted amino acid sequence of GIS indicates that it contains a C2H2 domain found in transcription factors of the TFIIIA class and is most similar to KNUCKLES and to the ZFP group of transcription factors (Figure 5; see Supplemental Figure 3 online) (Meissner and Michael, 1997; Payne et al., 2004).

To determine the pattern of *GIS* expression in wild-type plants, we first performed a quantitative RT-PCR analysis of transcript levels in different organs. In agreement with the phenotype of *gis* mutants, we found that *GIS* expression is low in rosette leaves and undetectable in roots. By contrast, *GIS* is most highly expressed in developing stems and branches, where expression levels are fairly consistent in successive paraclades (Figure 6A). To refine our analysis, we performed in situ hybridizations using *GIS*-specific probes on sections of developing inflorescence stems. This experiment confirmed that the gene is expressed broadly in the inflorescence, particularly in primary and secondary inflorescence meristems. It also showed that *GIS* is expressed strongly in the stem epidermis and in floral meristems (Figures 6B, 6D, and 6E).

In summary, we found that the pattern of *GIS* expression in the inflorescence, epidermis, and trichomes is consistent with the trichome phenotypes of overexpressors and loss-of-function mutants, although it could also support a wider role in the control of inflorescence maturation that is not apparent in the mutant but is suggested by the overexpression phenotype.

Epidermal Differentiation Is Less Responsive to GAs in *gis* Mutants

The epidermal phenotype of knockout mutants and overexpressors suggests that GIS acts in part to slow or prevent changes in the pattern of trichome initiation that are normally associated with shoot maturation, at least during reproductive development. Due to the known implication of GA signaling in phase change and trichome production, we investigated how fluctuations in GA levels would affect the *gis* phenotype. To this end, we submitted *gis* mutants to different levels of GA3 or paclobutrazole (PAC), which is a GA biosynthesis inhibitor. In addition to their effect on flowering and growth, GAs are known to promote trichome initiation on leaves, whereas PAC has the opposite effect (Chien and Sussex, 1996).

As expected, PAC applications induced late flowering and the shortening of internodes, indicating that the treatment was successful. By contrast, plants treated with GA flowered earlier and had a characteristic tall phenotype (Table 2).

We did not observe any significant difference in the mutant response to variations in GA signaling with respect to flowering time and leaf production (Table 2). However, there was a small but significant difference (*t* test, $P < 0.001$; $n = 20$) in the number of juvenile leaves produced by *gis* mutants compared with wild-type

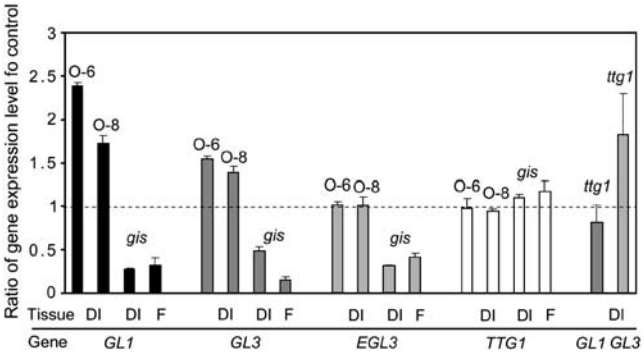

Figure 4. Quantitative PCR Analysis of Regulatory Genes Involved in Trichome Initiation in *gis* Mutants and *35S*:*GIS* Overexpressors.

Relative expression of *GL1*, *GL3*, *EGL3*, and *TTG1* in *gis* mutants, *35S*:*GIS*-overexpressing lines, and *ttg-1* mutants. Values represent the ratios of gene expression in a particular genotype to corresponding wild-type controls (dotted line indicates a ratio of 1, or identical expression to the wild type). Genotypes are indicated above each expression value. Tissues and genes used in the analysis are indicated under the *x* axis. O-6, *35S*:*GIS*-overexpressing line 6; O-8, *35S*:*GIS*-overexpressing line 8; DI, developing inflorescence shoots; F, flowers.

plants when high levels of PAC or GAs were applied: abaxial trichomes appeared noticeably later in the mutant on PAC- or GA-treated rosette leaves (Table 2), which suggested that the mutant was more sensitive to decreases and less to increases in GA levels. In line with these observations, we noticed that trichome initiation on later leaves was also less responsive to GA and more to PAC applications (Figure 7C). PAC also inhibited trichome initiation on cauline leaves and stems more strongly in the mutant than in wild-type plants, whereas trichome production was less induced if at all by GA applications (Figures 7A, 7B, and 7D). Taken together, these observations indicated that the mutant is altered in its sensitivity to GAs and suggested a role for GIS in the epidermal expression of vegetative phase change that is only revealed when GA signaling is altered.

GIS Acts Downstream of SPINDLY and Affects the Flowering Phenotype of *spindly* Mutants

To further probe the role of GAs in modulating its function, we investigated the interactions between GIS and components of

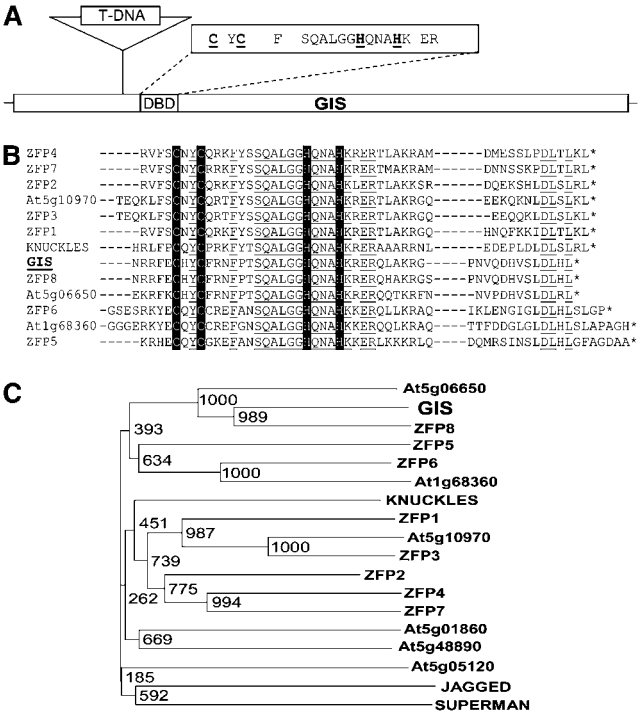

Figure 5. Structure of the *GIS* Gene and Similarity between GIS and Related Proteins.

(A) Schematic representation of the *GIS* gene. Conserved residues of the C2H2 domain are showed in an insert above the DNA binding domain. The C2H2 motif is underlined. DBD, DNA binding domain; T-DNA, T-DNA insertion.

(B) Alignment of the conserved regions of GIS and 12 most related proteins. Conserved residues are underlined, and the C2H2 motif is highlighted. Asterisks indicate stop codons.

(C) Phylogenetic tree of protein sequences similar to GIS. Bootstrap values are provided near the nodes.

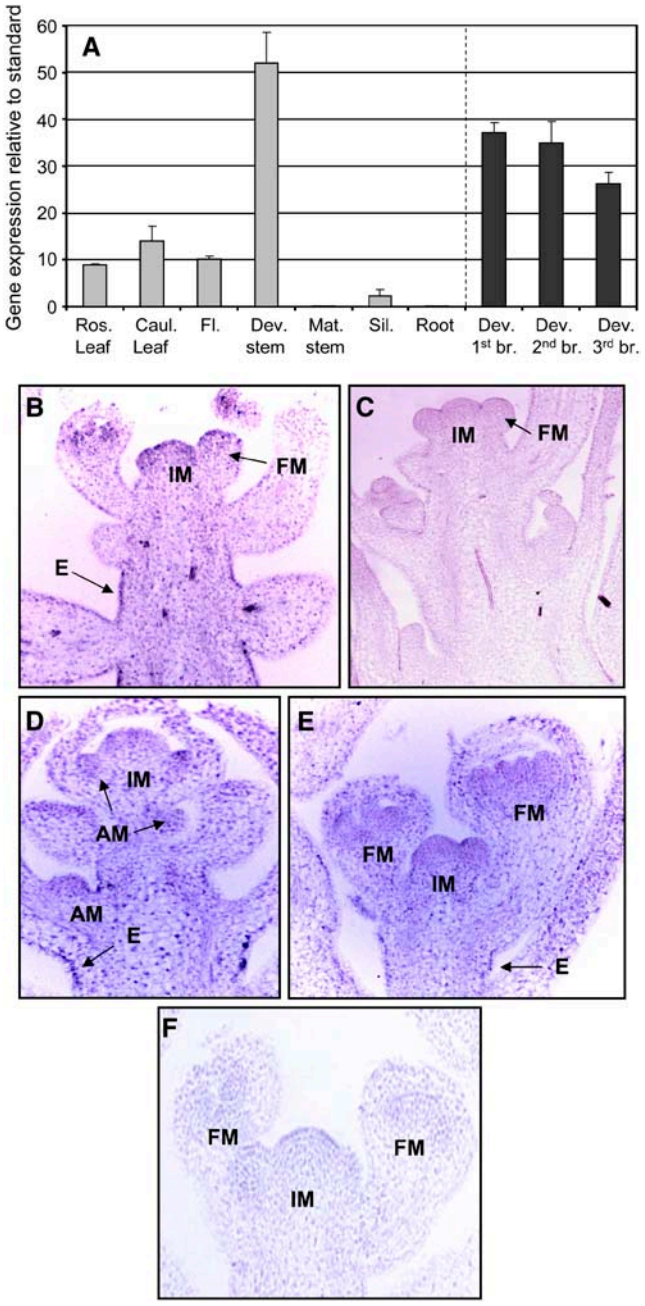

Figure 6. Expression Pattern of the *GIS* Gene.

(A) Quantitative RT-PCR analysis of *GIS* expression in different tissues of wild-type plants. Analysis of *GIS* expression in successive paraclades was performed in an independent experiment. All values are normalized using a common internal standard (*UBQ10*). Ros. Leaf, rosette leaf; Caul. Leaf, cauline leaf; Fl., flower; Dev. stem, developing main stem (1st internode); Mat. stem, fully elongated first internode of the main stem; Sil., silique; Dev. br., developing branch (paraclade).

(B) to **(F)** In situ hybridization of *GIS* probes to developing inflorescence shoot sections. *GIS* is expressed broadly in stems and strongly in inflorescence meristems (IM), axillary meristems (AM), floral meristems (FM), and in the epidermis (E). Antisense hybridizations (**[B]**, **[D]**, and **[E]**); control sense hybridizations (**[C]** and **[F]**).

Table 2. Developmental Effect of GA3 and PAC Applications on *gis* Mutants

		GA3 (μM)				PAC (mg/L)		
		0	10	100	20(*)	0	20	35
Leaf number at flowering	Wild type	12.0 (0.1)	11.9 (0.2)	10.4 (0.2)	9.0 (0.1)	-	-	-
	gis	11.8 (0.2)	11.9 (0.2)	10.1 (0.2)	9.1 (0.2)	-	-	-
Flowering time (d)	Wild type	27.8 (0.1)	27.1 (0.2)	26.6 (0.2)	25.4 (0.3)	29.6 (0.3)	32.3 (0.2)	35.4 (0.2)
	gis	27.5 (0.2)	26.7 (0.2)	26.2 (0.2)	25.1 (0.2)	29.4 (0.3)	32.6 (0.2)	35.7 (0.2)
First leaf with abaxial trichomes	Wild type	6.4 (0.1)	5.9 (0.1)	5.8 (0.1)	2.9 (0.1)	6.3 (0.1)	7.2 (0.1)	8.0 (0.1)
	gis	6.3 (0.1)	6.0 (0.1)	6.1 (0.1)	3.5 (0.1)	6.3 (0.1)	7.6 (0.1)	8.6 (0.1)

Values are averages and standard errors. (*), Applied to seedlings in growth medium before transfer to soil.

the GA signaling pathway. We first characterized genetic interactions between *GIS* and *SPINDLY* (*SPY*), which encodes a putative *O*-linked β-*N*-acetylglucosamine transferase playing a repressive role in GA signaling (Jacobsen et al., 1996). *spy* mutants display an early-flowering and accelerated growth phenotype that is largely reflective of constitutive GA response and bear many similarities with the phenotype of GA-treated plants (Jacobsen and Olszewski, 1993). They also transition between the juvenile and adult phases of vegetative development earlier than wild-type plants (Telfer et al., 1997) and produce more trichomes on rosette and inflorescence leaves (Chien and Sussex, 1996; Perazza et al., 1998). We therefore asked whether *GIS* was required for the expression of the vegetative and inflorescence trichome phenotypes in this mutant and constructed *gis spy* double mutants, using for this analysis *spy-3*, which is in the Col-0 background (Jacobsen and Olszewski, 1993).

We confirmed that *spy-3* mutants produce leaf abaxial trichomes earlier than control plants (Telfer et al., 1997) and found that, as in *spy-5* mutants, trichome production was elevated on leaves and stems (Perazza et al., 1998). By contrast, and consistent with the phenotype of GA-treated plants, we found that trichome densities on upper cauline leaves and paraclade stems of the *gis spy* mutant were similar to that of *gis* mutants (Figures 8A to 8C). Similarly to GA treatments, *SPY* loss-of-function caused a small increase in trichome density on lower inflorescence organs in *gis* mutants but more limited than in the wild-type background. Trichome production on the rosette leaves of double mutants was similar to that of *spy-3* and wild-type plants, although abaxial trichomes appeared slightly later on rosette leaves, as in *gis* seedlings that were established on GA-containing medium (Tables 1 and 2). Interestingly, whereas SPY loss-of-function had a negative effect on trichome branching on inflorescence stems, resulting in most trichomes being unbranched, *gis spy* double mutants had stem trichomes that were mostly three-branched, as in the *gis* mutants (Figure 8B). This observation, together with the trichome phenotype of late inflorescence organs in *gis* and *gis spy*, suggested that *gis* is largely epistatic to *spy*. Furthermore, the elevated trichome production on vegetative leaves and basal parts of the inflorescence in *gis spy* compared with *gis*, also seen in GA-treated *gis* mutants, indicated that GA signaling can promote trichome initiation locally, independently of GIS. Such a residual response to GA is also likely to be responsible for the overall increase in rosette leaf trichome branching that was observed on *gis spy* (data not shown) compared with *gis* mutants, as *spy* is known to promote trichome branching on leaves (Perazza et al., 1998).

The trichome phenotype of *gis spy* mutants could have been largely predicted from the observation of *gis* mutants to which GAs had been applied. We noticed, however, an important difference when we recorded the growth and development characteristics of the double mutant: in contrast with GA-treated *gis* mutants, which flowered at a similar time as GA-treated controls, *gis spy* mutants flowered significantly later than *spy* mutants (Table 1). A consistent yet smaller delay in flowering was also found in *gis*/+ *spy* heterozygotes. These observations suggested that GIS has a positive influence on flowering, independently of GA signaling, which can only be detected when repression by SPY of flowering is abolished. Interestingly, SPY is known to also act independently of GA signaling to repress flowering in long days (Tseng et al., 2004).

To further investigate how GIS loss-of-function affects the phenotype of *spy* mutants, we measured *GIS* expression in *spy* inflorescence stems. As shown on Figure 8F, we found that GIS expression was significantly higher in *spy-3*. This was in contrast with the expression of *SPY* in GIS loss-of-function mutants, which we found was unchanged compared with wild-type controls (data not shown). It therefore appeared that SPY is involved, directly or indirectly, in the repression of *GIS* and that derepression of *GIS* in *spy* mutants is associated with an increase in trichome density. Taken together with the phenotype of *gis spy* mutants, these observations strongly suggested that GIS acts downstream of SPY.

GIS Is GA Inducible and Its Induction Kinetics Are Similar to Those of *GL1*

The increase in *GIS* expression in the *spy-3* mutant raised the possibility that the gene is responsive to GA levels in the plants. We therefore set out to test the effect of GA on *GIS* expression by monitoring transcript levels over time after GA applications in wild-type plants and in the GA-deficient mutant *ga1-3* (Koornneef and Van Der Veen, 1980; Koornneef et al., 1985; Wilson et al., 1992; Sun and Kamiya, 1994). Plants were sprayed with 100 μM GA shortly after flowering, developing inflorescence stems were harvested, and *GIS* transcript levels were measured by quantitative PCR 4 and 6 h after treatment. In wild-type plants, GA applications had a small but significant effect on *GIS* expression (~1.5-fold increase) as soon as 4 h after treatment. However, this

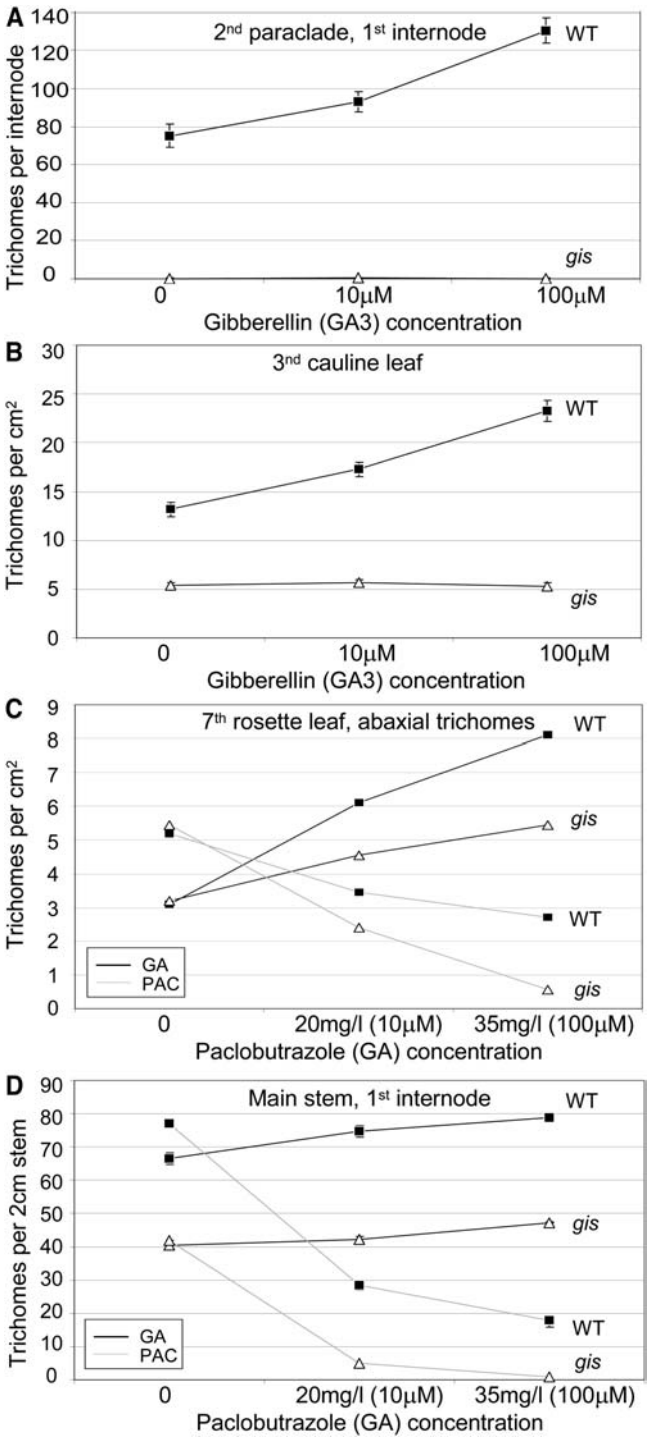

Figure 7. GAs and the *gis* Mutant Phenotype.

(A) and **(B)** Effects of GA applications at different concentrations on trichome initiation in *gis* mutants and controls.

(A) Trichome initiation on the first internode of the second branch.

(B) Trichome initiation on the abaxial side of the 3rd cauline leaf.

(C) and **(D)** Effects of GA and PAC applications on leaf (7th rosette leaf; **[C]**) and main stem trichome (1st internode; **[D]**) initiation of *gis* mutants and controls.

Squares, wild-type controls; triangles, *gis* mutants; black lines, GA treatments; gray lines, PAC treatments. GA and PAC treatments were done in separate experiments with a different set of control plants, and 20 plants were sampled for each condition. All values are averages, and error bars represent the standard error.

effect was much more pronounced in GA-treated *ga1-3* mutants, where GIS expression increased close to fourfold within the same time frame (Figure 8D). *GIS* transcript levels subsequently decreased in both backgrounds, while still remaining higher than in untreated controls. As a control, GA-insensitive *gai* mutants were submitted to the same treatments. In these mutants, GAI, a repressor of GA signaling belonging to the DELLA family, is constitutively active (Peng et al., 1997). In contrast with the effect seen in wild-type and *ga1-3* mutants, we did not detect any change in *GIS* expression in GA-treated *gai* mutants (Figure 8D).

Since we have shown that GL1 is likely to act downstream of GIS and since *GL1* expression levels are known to be regulated by GAs (Perazza et al., 1998), we investigated whether GA-mediated induction of *GL1* expression occurs within a similar time frame. Similarly to our analysis of *GIS* expression, we used quantitative PCR to determine *GL1* levels in GA-treated wild-type and *ga1-3* plants. Interestingly, we found that *GL1* induction also occurred within 4 h and decreased between 4 and 6 h after GA treatment. By contrast, *GL1* expression, like *GIS* expression, was not affected by GA applications in the *gai* mutant (Figure 8D).

These experiments showed that *GIS* is GA inducible and that changes in its expression depend on the activity of GAI. They also indicated that the response of *GL1* expression to variations in GA levels is similar in time to that of *GIS* and is also abolished by GAI repression.

GIS Mediates the Induction of *GL1* by GAs

The promotion of trichome initiation by GAs is thought to involve the regulation of *GL1* expression, as the gene is significantly induced by GA and repressed by PAC applications (Perazza et al., 1998). Since we placed GIS upstream of GL1 in the trichome initiation pathway and found that *GIS* and *GL1* were similarly responsive to GA treatments, we decided to test whether GIS is implicated in the activation of *GL1* expression by GAs. To this end, we compared *GL1* transcript levels in wild-type and *gis* mutant plants to which GAs had been applied. GA applications significantly induced *GL1* expression in wild-type plants: transcript levels increased between twofold and threefold within 4 h in developing main and secondary inflorescence shoots. By contrast, induction was significantly and reproducibly lower in *gis* mutants, where changes in *GL1* expression were still detectable but more limited (Figure 8D).

To further examine the role played by GIS in the regulation of *GL1* expression, we also compared *GL1* transcript levels in developing inflorescence shoots of *gis*, *gis spy*, and *spy* mutants. Consistent with the effect of GA applications on *GL1* expression, *GL1* transcripts were significantly more abundant in *spy*-3 than in wild-type plants. By contrast, *GL1* was more weakly expressed in *gis spy* mutants, and its expression level was comparable in the double mutant and in *gis* (Figure 8F).

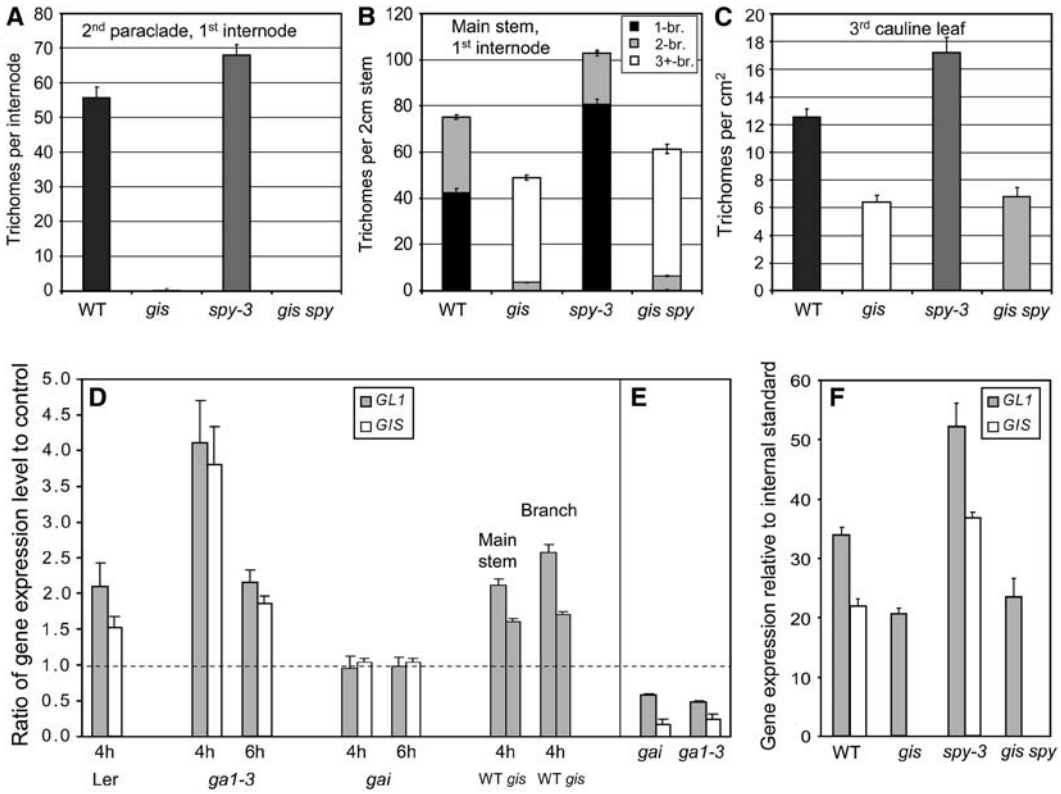

Figure 8. Genetic Interactions between *GIS* and *SPY* and the Effect of Variations in GA Signaling on *GIS* and *GL1* Expression.

(A) to **(C)** Trichome initiation phenotype of *spy*, *gis*, and *gis spy* mutants in branches **(A)**, main stems **(B)**, and cauline leaves **(C)**. The *gis* mutant is largely epistatic to *spy*. The trichome branching phenotype of the different mutants is illustrated in **(B)**. 1-br, one-branched (unbranched) trichomes; 2-br, two-branched trichomes; 3+-br, trichomes with three or more branches.

(D) to **(F)** Effect of variations in GA signaling on *GIS* and *GL1* expression.

(D) Effect of GA applications on *GIS* and *GL1* expression in developing inflorescences of *ga1-3*, *gai*, *gis*, and wild-type plants. GA3 (100 μM) was applied, and developing shoots were harvested 4 or 6 h later for gene expression analysis.

(E) *GIS* and *GL1* expression in the *gai* and *ga1-3* mutants. All values correspond to ratios of normalized gene expression values (obtained by quantitative RT-PCR) to appropriate controls. Averages of the ratios to mean control values are presented together with standard errors.

(F) *GIS* and *GL1* expression in developing inflorescence stems of *spy*, *gis*, and *gis spy* mutants and control plants measured by quantitative RT-PCR. All values are normalized using a common internal standard (*UBQ10*).

Taken together, these results suggested that GIS mediates the induction of *GL1* expression by GAs in inflorescence shoots.

Repression of Trichome Initiation Involves GAI and Is Independent of *GIS* Expression Levels

We showed that GIS is sufficient for inducing trichome initiation and *GL1* expression in transgenic plants and that it also mediates its induction by GAs in developing inflorescence shoots. We also showed that *GIS* and *GL1* induction by GAs depends on GAI activity and does not occur when the repressor is active.

Trichome initiation is known to require normal levels of GA signaling, since the *ga1-3* mutant, which is severely deficient in the production of GAs, is near-glabrous. The *gai* signaling mutant is also deficient in trichome production, especially on inflorescence organs (Figure 3D), although it still produces leaf trichomes. In addition to its effect on initiation, GA deficiency also leads to a drop in *GL1* transcript levels (Perazza et al., 1998). Therefore, whereas increases in levels of GA or GA signaling induce *GL1* and trichome production, the opposite causes the repression of *GL1* expression and inhibits trichome initiation. Since positive regulation by GA, which is antagonized by GAI, involves the induction of *GIS* expression, we asked whether negative regulation reciprocally proceeds through the repression of *GIS* expression and if this repression is mediated by GAI.

To this end, we first measured *GIS* expression in developing inflorescence shoots of the *ga1-3* and *gai* mutants and found that, in agreement with our hypothesis, *GIS* is expressed at significantly lower levels in the mutants than in wild-type plants. We also found that *GL1* was repressed in both mutants (Figure 8E). To test whether *GIS* downregulation is necessary for repression of trichome initiation, we overexpressed *GIS* in the *ga1-3* and *gai* mutants. Surprisingly, we found that *GIS* overexpression does not have an effect on trichome initiation in either *ga1-3* or *gai*. No

increase in trichome density was noticeable on leaves, stems, or flowers of *35S*:*GIS gai* plants, and carpels did not produce ectopic trichomes (Figure 3D). *ga1-3* plants overexpressing *GIS* displayed a similar phenotype (see Supplemental Figure 3 online). To test whether *GIS* expression levels in transgenic plants were sufficient to induce the overexpression phenotype, we sprayed *35S*:*GIS ga1-3* plants with 100 μM GA. This treatment restored the overexpression phenotype normally seen in a wild-type background (data not shown). We also verified *GIS* expression levels in *35S*:*GIS gai* and *35S*:*GIS ga1-3* transgenic lines and found that *GIS* was indeed overexpressed to significant levels (27- and 442-fold, respectively, in the lines we tested).

The phenotype of *GIS* overexpressing *gai* and *ga1-3* plants indicated that GAI-mediated repression of trichome initiation is independent of *GIS* expression levels. To test whether it was also independent of *GL1* expression levels, we measured *GL1* transcript levels in *35S*:*GIS gai*, *35S*:*GIS ga1-3*, and control plants. We found that *GL1* was still repressed in spite of high levels of *GIS* expression in transgenic plants and in fact was expressed at similar levels in *35S*:*GIS gai*, *35S*:*GIS ga1-3*, and control plants (see Supplemental Figure 4 online).

Therefore, repression of trichome initiation and *GL1* expression in the absence of GA signaling, while it involves the GAI-mediated downregulation of *GIS* expression, occurs independently of *GIS* expression levels.

DISCUSSION

We report the identification of a putative C2H2 transcription factor, GIS, which regulates several aspects of shoot maturation in *Arabidopsis*. The analysis of overexpressors and loss-of-function mutants indicates that GIS plays a central role in the control of trichome initiation during inflorescence development. GIS also plays a role in the regulation of epidermal differentiation during the vegetative phase, although this function only becomes apparent when GA signaling is altered in the plant. The phenotype of *gis spy* double mutants indicates that GIS also modulates the repressive effect exerted by SPY on flowering. Through the analysis of gene expression profiles, genetic interactions, and effects of modulating GA levels in the plant, we have found that GIS acts downstream of the GA signaling pathway and controls epidermal differentiation by modulating the activity of one or more cognate regulators of trichome initiation.

Role of GIS in Shoot Maturation

The phenotype of loss-of-function mutants and overexpressors indicates that GIS promotes epidermal differentiation during inflorescence development by inducing trichome initiation. Based on the extent of trichome loss in the mutant, it appears that GIS plays a predominant role in inflorescence stems (Figures 2A to 2D), which is consistent with its strong expression in stem epidermal cells (Figure 6).

Our analysis of the genetic interactions between *GIS*, *GL1*, *GL3*, and *TTG1* and of gene expression also suggests that GIS acts upstream of the trichome initiation complex and that it modulates the activity of the complex through a direct or indirect transcriptional mechanism.

While the gain-of-function and loss-of-function phenotypes and gene expression data argue that GIS is an activator of inflorescence trichome initiation, the occasional appearance of rosettes on overexpressors could suggest that GIS is more generally repressing inflorescence shoot maturation and controls the timing of trichome initiation rather than initiation itself. This scenario could be supported by the broad expression of GIS during inflorescence development, which would be compatible with a regulatory role that goes beyond epidermal differentiation. Whether GIS plays a direct or indirect role in promoting trichome initiation should become clearer once its immediate targets are identified.

Regardless of this mechanism, the residual production in *gis* of trichomes on early inflorescence organs where the gene is normally expressed suggests that other regulators act in parallel to control trichome initiation. The regulation of these redundant factors is also likely to be important to the progression of the epidermal differentiation program, and it will be interesting to determine whether they respond to distinct developmental signals. In this respect, it will be sensible to define the function of C2H2 proteins that are most closely related to GIS, as the similarity in sequence between the homologs is suggestive of redundancy.

The role of GIS in other aspects of shoot maturation appears to be more complex. The timings of vegetative phase change and flowering are not affected in the mutant under normal conditions, although the results of exogenous GAs and PAC applications imply that abaxial trichome initiation requires higher GA levels in the mutant than in wild-type plants. This observation is in agreement with the phenotype of *gis spy* double mutants and suggests that GIS plays a role in promoting abaxial trichome production during the juvenile–adult transition (which would support a role for GIS as an activator of trichome initiation throughout the plant). An interesting finding is that GIS loss of

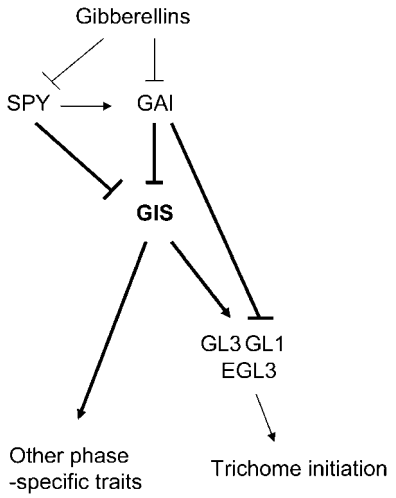

Figure 9. Proposed Model of the Regulation of Inflorescence Trichome Production and Shoot Maturation by GIS in *Arabidopsis*.

Arrows in bold correspond to relationships that were investigated in this study, and they reflect either genetic analysis, gene expression data, or both.

function also affects flowering time in the *spy* background. This effect appears to be independent of GA levels as GA- and PAC-treated *gis* mutants do not flower significantly earlier or later than wild-type plants. The two results are not necessarily inconsistent, as SPY has recently been shown to be implicated in the GA-independent control of flowering under long days through its interactions with GIGANTEA (Tseng et al., 2004). GIS could also play a role in this pathway by antagonizing the repressive effect of SPY on flowering. To examine this possibility, we are currently exploring genetic interactions between *gis*, *gigantea*, and *constans*.

A positive role by GIS in the regulation of flowering under long days and in the regulation of vegetative phase change by GA is in apparent contradiction with the phenotype of GIS overexpressors. While in agreement during inflorescence development, the loss-of-function and gain-of-function phenotypes seem inconsistent during the vegetative phase, as both mutant and overexpressors are, under inductive conditions, delayed in phase transitions. One possibility is that overexpression of GIS results in a dominant-negative effect that equates loss of function in vegetative organs but not in inflorescence organs, for example, through the inhibition of a regulatory complex that only forms before flowering. Alternatively, aspects of the overexpression phenotype that are not mirrored in the mutant could be an artifact of ectopic expression. Regardless of what causes the preflowering phenotype of *GIS* overexpressors, it is clear that GIS is implicated in the control of phase change during vegetative development and acts by integrating GA-dependent and -independent signals. Identification of proteins interacting with GIS and functional characterization of close homologs should bring further definition to its mode of action during the vegetative phase.

GIS and GA Signaling

The lower sensitivity of *gis* mutants to GAs, indicated by the result of GA and PAC applications, implies that GIS plays a role in modulating GA signaling in the regulation of shoot maturation. Such a role is further suggested by genetic interactions between *GIS*, *GA1*, *GAI*, and *SPY*. In particular, we found that the inflorescence phenotype of *gis spy* is most similar to that of *gis* mutants and that *GIS* is upregulated in *spy*, which suggests that GIS acts downstream of SPY. The fact that *gis* strongly attenuates the induction of *GL1* by GAs indicates that the mode of action of GIS is in part to mediate GA signaling in the control of *GL1* expression. In this, GIS is antagonized by GAI, which also represses the induction of trichome initiation when *GIS* is overexpressed in the *gai* mutant background. The impact of GAI on the competence of the plant to respond to GIS is reminiscent of the effect of the *ga1-3* mutation on *LEAFY* overexpression, although in this case, the overexpressors still respond, albeit weakly, to LEAFY activity (Blazquez et al., 1998).

In summary, GIS is required for the induction of trichome initiation through its role in regulating *GL1* expression, but its downregulation in the absence of GA signaling is not necessary for the repression of trichome initiation and *GL1* expression. These observations lead us to a model of GA control over trichome initiation, according to which GIS acts downstream of SPY but at the same step as GAI (and possibly other DELLA proteins) in the regulation of GL1 to influence trichome initiation (Figure 9).

In conclusion, the identification of *GIS* is a first step in the elucidation of mechanisms through which GAs control cellular differentiation and epidermal aspects of phase change. Further definition of these mechanisms and of the interaction between GA-dependent and -independent pathways is likely to come from continued analysis of the biological roles of GIS and other members of its clade.

METHODS

Plant Material and Growth Conditions

Arabidopsis thaliana ecotype Col-0 was used as a control for most experiments in this study. The *gl1-1*, *ttg-1*, *gai-1*, *ga1-3*, and *spy-3* mutants were obtained from the Nottingham Arabidopsis Stock Centre, and the *gl3-1* mutant was kindly proved by Alan Lloyd. The *gis spy-3* double mutants were selected out of an F2 population by selection on Murashige and Skoog medium containing sulfadiazine and PAC. Double mutants were confirmed by selfing the selected F2s and ensuring all progenies were resistant to both sulfadiazine and PAC. Plants of the Lansdsberg *erecta* ecotype were grown as a control whenever necessary. In all trichome counting experiments, the plants were grown under a 16-h-light (90 $\mu E \cdot cm^{-2} \cdot s^{-2}$; 21°C) and 8-h-dark (18°C) cycle. Short-day experiments were performed with 8-h-light (90 $\mu E \cdot cm^{-2} \cdot s^{-2}$; 21°C) and 16-h-dark (18°C) cycles. Sepal trichome numbers were recorded ~35 d after sowing, when the plant reached ~11 cm in size, on three apical flowers per plant. Leaf trichomes were counted when the leaves had fully expanded, on a 1-cm^{-2} area in the middle of the leaf. When the main inflorescence stem reached ~18 cm in size, the total number of trichomes was counted on the first two to three branches, and on one to three basal internodes, depending on the experiment. At least 20 plants were used for trichome count analysis for each of the treatment × genotype combinations. All the experiments were repeated at least once.

Isolation of a GIS Knockout Mutant

A transgenic line (catalogue number 423G08) carrying a T-DNA insertion in *GIS* was identified in the GABI-Kat line collection (Rosso et al., 2003). Homozygous mutants were selected by ensuring that all of their progenies were resistant to sulfadiazine (5.2 mg/L). Presence of the T-DNA insertion was confirmed by PCR using gene-specific primers (5′ primer, 5′-GTTCGCGTTTGTGAGCGTTTT-3′; 3′ primer, 5′-TACGAAAATGCCACCCATCCA-3′; and a T-DNA insertion primer, (5′-GGGCTACACTGAATTGGTAGCTC-3′).

GA and PAC Applications for Sensitivity Assays and Gene Expression Analysis

GA3 (Sigma-Aldrich) was used for all GA applications. Wild-type and *gis* mutant plants were grown on soil until the first three leaves had emerged and then sprayed with GA3 solutions. Spraying was performed twice a week until the plants reached a size of ~13 cm. Control plants for each treatment were sprayed with a mock solution without GA3.

For experiments aimed at measuring induction of gene expression in response to GA, *gai*, *gal-3*, *gis*, and control plants were grown on soil until young inflorescence shoots or paraclades had reached a size of 2 to 3 cm. The plants were then sprayed with either 100 μM GA3 or a mock solution, and the shoots were harvested 4 or 6 h after treatment for RNA extraction.

Aqueous solutions of PAC (Sigma-Aldrich) were applied to soil-grown plants by soaking the pots for 2 d when the plants had reached the four-leaf stage, unless stem trichome density was to be measured, in which case PAC was applied at the eight-leaf stage. The PAC solution was then

removed from trays, and normal watering was resumed. Trichome data were recorded ~35 d after sowing.

Molecular Biology

RNA Extraction and Real-Time RT-PCR

Plant RNA was extracted using TRIzol reagent (Invitrogen) according to the manufacturer's protocol. Pooled samples from at least eight plants were used for extractions. Gene-specific primer sequences went as follows: *GIS*, 5′-TTCATGAACGTCGAATCCTTCTC-3′ and 5′-ACGAATGGGTTTAGGGTTCTTATCT-3′; *UBQ10*, 5′-GGTTCGTACCTTTGTCCAAGCA-3′ and 5′-CCTTCGTTAAACCAAGCTCAGTATC-3′; *GL1*, 5′-CGACTCTCCACCGTCATTGTT-3′ and 5′-TTCTCGTAGATATTTTCTTGTTGATGATG-3′; *GL3*, 5′-GGTACCACAGAACATATTACGGAAGA-3′ and 5′-CAAGAACGTTGTCGATGTGATAATC-3′; *EGL3*, 5′-TTGATCCCTTAAGTGACGATAAATACA-3′ and 5′-CAAACCCGCTAGTAGAAGTTGTTG-3′; *TTG1*, 5′-CCGTCTTTGGGAAATTAACGAA-3′ and 5′-GCTCGTTTTGCTGTTGTTGAGA-3′. The primers were designed to include, when possible, an intron-exon boundary in the amplicon. cDNA was synthesized from 5 μg of total RNA using Superscript reverse transcriptase (Invitrogen) and random hexamer primers in a 40-μL reaction according to the manufacturer's instructions. For real-time PCR, the cDNAs were diluted to 200 μL, and 3.5 μL was added to 12.5 μL of SYBR-green PCR mix (Applied Biosystems) and 4.5 μL of each primer (198 nM final concentration) in triplicate 25-μL reactions. PCR and detection were performed using an ABI Prism 7000 thermal cycler (Applied Biosystems), using the following cycling conditions: 95°C for 10 min, followed by 40 cycles of 95°C for 15 s and 60°C for 1 min. Optimization experiments were performed to establish the optimal concentration of primers. Melting curve analysis and gel electrophoresis of the PCR products were used to confirm the absence of nonspecific amplification products. *UBQ10* transcripts were used as an endogenous control to normalize expression of the other genes. *UBQ10* was chosen as the housekeeping gene because its expression appeared to be most stable between different tissues and treatments (Gan et al., 2005). Relative expression levels were calculated by subtracting the threshold cycle (Ct) values for *UBQ10* from those of the target gene (to give ΔCt) and then calculating $2^{-\Delta Ct}$. RT-PCR experiments were performed on two independent samples.

Cloning

For all cloning experiments (35S:*GIS*, *GIS*-RNAi, *GIS* promoter:β-glucuronidase fusion [p*GIS*:GUS], and 35S:*R*), except for those involving the maize (*Zea mays*) *R* gene, all sequences were first inserted into the pENTR-1A vector (Invitrogen) before being recombined into an appropriate destination vector using the Gateway LR reaction (Invitrogen). All destination vectors were obtained from VIB (Flanders Interuniversity Institute for Biotechnology). pH2GW7 was used for preparing the 35S:*GIS* construct, pK7GWIWG2(II) for the *GIS*-RNAi construct, and pHGWFS7 for the construction of the p*GIS*:GUS fusion construct.

For all these cloning experiments, gene-specific fragments were first PCR amplified from cDNA (35S:*GIS* and *GIS*-RNAi) or genomic DNA (p*GIS*:GUS) using primers containing *Sal*I and *Not*I restriction sites, purified using a gel extraction kit (Clontech) before restriction and cloning. The following primers were used: *GIS* overexpression, 5′-TTTCTCAGTCGACCGCCCAGTCTTTTTATCTCTC-3′ and 5′-TCATTCAGCGGCCGCACACATCGTGCCGTTTCTT-3′; *GIS*-RNAi, 5′-CATTGTCGACTTACCGTCATTACCCGTCGT-3′ and 5′-TCGCGGCCGCACACATCGTGCCGTTTCTT-3′. A 1.6-kb genomic fragment upstream of the start codon in *GIS* was amplified using the primers 5′-ATCTTGGTCGACTGCACACACTTTTATGGCAAA-3′ and 5′-CTAATGGCGGCCGCGAGAGATAAAAAGACTGGGCG-3′ for preparing the p*GIS*:*GUS* construct.

The *R* gene was PCR amplified from maize cDNA using the primers 5′-CTGAGTCGACATCGAGTTGTTGTACTCTTCGCAGA-3′ and 5′-TCGATCCCGCGGCCGCTTCCATGCCCGTCGATGTCCAAA-3′, cloned first into the pMEN065 vector, then subcloned into the pBI101 vector.

All binary vector constructs were introduced into *Agrobacterium tumefaciens* strain GV3101 by electroporation. *Agrobacterium*-mediated transformation of all *Arabidopsis* genotypes was performed using the floral dip method (Clough and Bent, 1998), and transgenic seeds were selected using hygromycin (35S:*GIS* and p*GIS*:*GUS*) or kanamycin (*GIS*-RNAi and 35S:*R*).

In Situ Hybridization

Nonradioactive in situ hybridization was performed according to a published protocol (Long and Barton, 1998). For synthesis of the antisense and sense *GIS* RNA probes, a gene-specific fragment was amplified using the same primers as for generating the *GIS*-RNAi constructs (see above) and cloned into pGEM-T Easy vector (Promega). The resulting plasmid served as template for in vitro transcription, which was performed using the DIG RNA labeling kit (Roche Molecular Biochemicals).

Phylogenetic Analysis

Phylogenetic trees were generated using alignments of complete predicted protein sequences using the ClustalX program (Figure 5; see Supplemental Figure 3 online) (Thompson et al., 1997). The same program was used to produce alignments of conserved regions of the proteins (Figure 5). Alignment parameters were as follows: gap opening penalty = 10 and gap extension penalty = 0.2. Gonnet weight matrices were selected as a way to determine the similarity of nonidentical amino acids. The trees were generated using the neighbor-joining method (Saitou and Nei, 1987) with a number of bootstrap replicates set at 1000.

Accession Numbers

Sequence data from this article can be found in the GenBank/EMBL data libraries under the following accession numbers: *GIS*, At3g58070; *GL1*, At3g27920; *GL3*, At5g41315; *EGL3*, At1g63650; *TTG1*, At5g24520; *UBQ10*, At4g05320.

Supplemental Data

The following materials are available in the online version of this article.

Supplemental Figure 1. *GIS* Expression in T-DNA and RNAi Lines.

Supplemental Figure 2. Developmental Regulation of Trichome Initiation on Wild-Type Inflorescence Organs.

Supplemental Figure 3. Alignment of the Predicted Amino Acid Sequences of Transcription Factors Related to GIS.

Supplemental Figure 4. Effect of *GIS* Overexpression on the *ga1-3* Phenotype and on *GL1* Expression Levels in *ga1-3* and *gai*.

ACKNOWLEDGMENTS

We thank Ottoline Leyser for useful comments on the manuscript, the Garfield Weston Foundation for funding Y.G.'s work, and all the scientists at Mendel Biotechnology who have contributed, directly or indirectly, to this work.

Received January 30, 2006; revised March 13, 2006; accepted March 30, 2006; published May 5, 2006.

REFERENCES

Berardini, T.Z., Bollman, K., Sun, H., and Poethig, R.S. (2001). Regulation of vegetative phase change in *Arabidopsis thaliana* by cyclophilin 40. Science **291,** 2405–2407.

Blazquez, M.A., Green, R., Nilsson, O., Sussman, M.R., and Weigel, D. (1998). Gibberellins promote flowering of *Arabidopsis* by activating the LEAFY promoter. Plant Cell **10,** 791–800.

Chien, J.C., and Sussex, I.M. (1996). Differential regulation of trichome formation on the adaxial and abaxial leaf surfaces by gibberellins and photoperiod in *Arabidopsis thaliana* (L.) Heynh. Plant Physiol. **111,** 1321–1328.

Clarke, J.H., Tack, D., Findlay, K., Van Montagu, M., and Van Lijsebettens, M. (1999). The SERRATE locus controls the formation of the early juvenile leaves and phase length in *Arabidopsis.* Plant J. **20,** 493–501.

Clough, S.J., and Bent, A.F. (1998). Floral dip: A simplified method for Agrobacterium-mediated transformation of *Arabidopsis thaliana.* Plant J. **16,** 735–743.

Evans, M.M., and Poethig, R.S. (1995). Gibberellins promote vegetative phase change and reproductive maturity in maize. Plant Physiol. **108,** 475–487.

Gan, Y., Filleur, S., Rahman, A., Gotensparre, S., and Forde, B.G. (2005). Nutritional regulation of ANR1 and other root-expressed MADS-box genes in *Arabidopsis thaliana.* Planta **222,** 730–742.

Gazzarrini, S., Tsuchiya, Y., Lumba, S., Okamoto, M., and McCourt, P. (2004). The transcription factor FUSCA3 controls developmental timing in *Arabidopsis* through the hormones gibberellin and abscisic acid. Dev. Cell **7,** 373–385.

Groot, E.P., and Meicenheimer, R.D. (2000). Comparison of leaf plastochron index and allometric analyses of tooth development in *Arabidopsis thaliana.* J. Plant Growth Regul. **19,** 77–89.

Hempel, F.D., and Feldman, L.J. (1994). Bi-directional inflorescence development in *Arabidopsis thaliana*: Acropetal initiation of flowers and basipetal initiation of paraclades. Planta **192,** 276–286.

Hunter, C., Sun, H., and Poethig, R.S. (2003). The *Arabidopsis* heterochronic gene ZIPPY is an ARGONAUTE family member. Curr. Biol. **13,** 1734–1739.

Jacobsen, S.E., Binkowski, K.A., and Olszewski, N.E. (1996). SPINDLY, a tetratricopeptide repeat protein involved in gibberellin signal transduction in *Arabidopsis.* Proc. Natl. Acad. Sci. USA **93,** 9292–9296.

Jacobsen, S.E., and Olszewski, N.E. (1993). Mutations at the SPINDLY locus of *Arabidopsis* alter gibberellin signal transduction. Plant Cell **5,** 887–896.

Koornneef, M., and Van Der Veen, J.H. (1980). Induction and analysis of gibberellin sensitive mutants in *Arabidopsis thaliana.* Theor. Appl. Genet. **58,** 257–263.

Koornneef, M., Elgersma, A., Hanhart, C.J., van Loenen-Martinet, E.P., van Rign, and Zeevaart, J.A.D. (1985). A gibberellin insensitive mutant of *Arabidopsis thaliana.* Physiol. Plant. **65,** 33–39.

Larkin, J.C., Oppenheimer, D.G., Lloyd, A.M., Paparozzi, E.T., and Marks, M.D. (1994). Roles of the GLABROUS1 and TRANSPARENT TESTA GLABRA genes in *Arabidopsis* trichome development. Plant Cell **6,** 1065–1076.

Lloyd, A.M., Walbot, V., and Davis, R.W. (1992). *Arabidopsis* and *Nicotiana anthocyanin* production activated by maize regulators R and C1. Science **258,** 1773–1775.

Long, J.A., and Barton, M.K. (1998). The development of apical embryonic pattern in *Arabidopsis.* Development **125,** 3027–3035.

Meissner, R., and Michael, A.J. (1997). Isolation and characterisation of a diverse family of *Arabidopsis* two and three-fingered C2H2 zinc finger protein genes and cDNAs. Plant Mol. Biol. **33,** 615–624.

Payne, C.T., Zhang, F., and Lloyd, A.M. (2000). GL3 encodes a bHLH protein that regulates trichome development in *Arabidopsis* through interaction with GL1 and TTG1. Genetics **156,** 1349–1362.

Payne, T., Johnson, S.D., and Koltunow, A.M. (2004). KNUCKLES (KNU) encodes a C2H2 zinc-finger protein that regulates development of basal pattern elements of the *Arabidopsis* gynoecium. Development **131,** 3737–3749.

Peng, J., Carol, P., Richards, D.E., King, K.E., Cowling, R.J., Murphy, G.P., and Harberd, N.P. (1997). The *Arabidopsis* GAI gene defines a signaling pathway that negatively regulates gibberellin responses. Genes Dev. **11,** 3194–3205.

Perazza, D., Vachon, G., and Herzog, M. (1998). Gibberellins promote trichome formation by up-regulating GLABROUS1 in *Arabidopsis.* Plant Physiol. **117,** 375–383.

Prigge, M.J., and Wagner, D.R. (2001). The *Arabidopsis* serrate gene encodes a zinc-finger protein required for normal shoot development. Plant Cell **13,** 1263–1279.

Riechmann, J.L., et al. (2000). *Arabidopsis* transcription factors: Genome-wide comparative analysis among eukaryotes. Science **290,** 2105–2110.

Rosso, M.G., Li, Y., Strizhov, N., Reiss, B., Dekker, K., and Weisshaar, B. (2003). An *Arabidopsis thaliana* T-DNA mutagenized population (GABI-Kat) for flanking sequence tag-based reverse genetics. Plant Mol. Biol. **53,** 247–259.

Saitou, N., and Nei, M. (1987). The neighbor-joining method: A new method for reconstructing phylogenetic trees. Mol. Biol. Evol. **4,** 406–425.

Sun, T.P., and Kamiya, Y. (1994). The *Arabidopsis* GA1 locus encodes the cyclase ent-kaurene synthetase A of gibberellin biosynthesis. Plant Cell **6,** 1509–1518.

Telfer, A., Bollman, K.M., and Poethig, R.S. (1997). Phase change and the regulation of trichome distribution in *Arabidopsis thaliana.* Development **124,** 645–654.

Telfer, A., and Poethig, R.S. (1998). HASTY: A gene that regulates the timing of shoot maturation in *Arabidopsis thaliana.* Development **125,** 1889–1898.

Thompson, J.D., Gibson, T.J., Plewniak, F., Jeanmougin, F., and Higgins, D.G. (1997). The ClustalX windows interface: Flexible strategies for multiple sequence alignment aided by quality analysis tools. Nucleic Acids Res. **24,** 4876–4882.

Tseng, T.S., Salome, P.A., McClung, C.R., and Olszewski, N.E. (2004). SPINDLY and GIGANTEA interact and act in *Arabidopsis thaliana* pathways involved in light responses, flowering, and rhythms in cotyledon movements. Plant Cell **16,** 1550–1563.

Walker, A.R., Davison, P.A., Bolognesi-Winfield, A.C., James, C.M., Srinivasan, N., Blundell, T.L., Esch, J.J., Marks, M.D., and Gray, J.C. (1999). The TRANSPARENT TESTA GLABRA1 locus, which regulates trichome differentiation and anthocyanin biosynthesis in *Arabidopsis*, encodes a WD40 repeat protein. Plant Cell **11,** 1337–1350.

Wilson, R.N., Heckman, J.W., and Somerville, C.R. (1992). Gibberellin is required for flowering in *Arabidopsis thaliana* under short days. Plant Physiol. **100,** 403–408.

Zhang, F., Gonzalez, A., Zhao, M., Payne, C.T., and Lloyd, A. (2003). A network of redundant bHLH proteins functions in all TTG1-dependent pathways of *Arabidopsis.* Development **130,** 4859–4869.